

1
2
3
4
5
6
7
8
9
10
11
12
13
14
15
16
17
18
19
20
21
22
23
24
25
26
27
28
29

Mitochondrial content is preserved throughout disease progression in the *mdx* mouse model of Duchenne muscular dystrophy, regardless of taurine supplementation

Robert G. Barker¹, Victoria L. Wyckelsma¹, Hongyang Xu¹ and Robyn M. Murphy¹

¹Department of Biochemistry and Genetics, La Trobe Institute for Molecular Science La Trobe University, Melbourne, VIC 3086, Australia.

Correspondence:
Assoc Prof Robyn M. Murphy,
Department of Biochemistry and Genetics,
La Trobe Institute for Molecular Science,
La Trobe University, Melbourne,
Victoria, 3086 Australia,
Telephone: +61-3-9479-2302;
Email: r.murphy@latrobe.edu.au

Running title: Mitochondria in *mdx* mice

Keywords: DMD; *mdx* mouse; Taurine; Skeletal Muscle; Animal Model; mitochondria

30 **Abstract**

31 Mitochondrial dysfunction is a pathological feature of Duchenne muscular dystrophy (DMD),
32 a debilitating and fatal neuromuscular disorder characterised by progressive muscle wasting
33 and weakness. Mitochondria are a source of cellular ATP, involved in Ca²⁺ regulation and
34 apoptotic signalling. Ameliorating aberrant mitochondrial function has therapeutic
35 potential for reducing DMD disease severity. The dystrophic *mdx* mouse exhibits peak
36 muscle damage at 21-28d which stabilises after 8 weeks. The amino acid taurine is
37 implicated in mitochondrial health and function, with endogenous concentrations low when
38 measured during the cycle of peak muscle damage in *mdx* mice. Using whole soleus and EDL
39 muscle homogenates from 28- and 70-d *mdx* mice there was no change in native state
40 mitochondrial complexes using Blue Native-PAGE. NADH:ubiquinone oxidoreductase
41 subunit-A9 (NDUFA9) protein abundance was lower in soleus muscle of 28 and 70 d *mdx*
42 mice and EDL muscle of 70 d *mdx* mice compared to same muscles in WT (C57BL10/ScSn)
43 animals. There were age dependant increases in both NDUFA9 protein abundance and
44 citrate synthase activity in soleus muscles of *mdx* and WT mice. There was no change in
45 abundances of mitochondrial dynamics proteins mitofusin 2 (Mfn2) and mitochondrial
46 dynamics protein 49 (MiD49). Taurine administration essentially did not affect any
47 measurements of mitochondria. Collectively these findings suggest mitochondrial content
48 and dynamics are not reduced in the *mdx* mouse regardless of disease severity. We also
49 elucidate that taurine affords no significant benefit to mitochondrial content or dynamics in
50 the *mdx* mouse at either 28 or 70 d.

51 **Abbreviations** :Blue native polyacrylamide gel electrophoresis (BN-PAGE); bovine serum
52 albumin (BSA); citrate synthase (CS); cytochrome C oxidase subunit IV (COX IV); Days (d);
53 Development Studies Hybridoma Bank (DSHB); Duchenne muscular dystrophy (DMD);
54 extensor digitorum longus (EDL); mitochondrial ATP production rate (MAPR); mitochondrial
55 dynamics protein 49 (MiD49); mitofusin 2 (Mfn2); NADH:ubiquinone oxidoreductase
56 subunit-A9 (NDUFA9); oxidative phosphorylation (OXPHOS); phosphate buffered saline
57 (PBS); phosphate buffered saline with 0.025% Tween (PBST); reactive oxygen species (ROS);
58 sarcoplasmic reticulum (SR); SR-calcium ATPase (SERCA); standard deviation (SD); taurine
59 (tau); Tris-buffered, saline-Tween (TBST); Wild type (WT, C57/BL10ScSn)

60 **Introduction**

61 Duchenne Muscular Dystrophy (DMD) is a debilitating, progressive and ultimately fatal
62 neuromuscular disorder affecting approximately 1:3600 live male births (5). Caused by the
63 absence of the protein dystrophin and the subsequent weakening of the sarcolemma, an
64 influx of extracellular Ca^{2+} precedes myofibre necrosis and subsequently progressive muscle
65 wasting and weakness with age (1). The dystrophin deficient *mdx* mouse is a well-
66 established animal model of DMD and exhibits many of the pathophysiological symptoms
67 associated with the disorder (12). It doesn't, however, experience progressive muscle
68 wasting and weakness but rather exhibits an age dependant disease severity, peaking at 21-
69 28 (d)ays at which time it most closely mimics the severity of DMD, before undergoing
70 successful muscle regeneration and stabilising into adulthood (> 8 weeks)(12).

71 The structural hypothesis for damage in DMD is centred on this Ca^{2+} entry and is widely
72 recognised to precede many of the pathological features seen with DMD (1). Intracellular
73 Ca^{2+} is continuously sequestered into the specialised membrane bound store, the
74 sarcoplasmic reticulum (SR) by the SR-calcium ATPase (SERCA), and hence has a reliance on
75 ATP supply for continued function. A further key aspect of dystrophic muscle is the
76 increased requirement for muscle regeneration as the tissue attempts to repair itself, and
77 this is another significant ATP consuming pathway in the cell.

78 Mitochondria are the source of cellular energy, producing ATP through a series of five
79 multimeric enzyme complexes termed oxidative phosphorylation (OXPHOS) and play an
80 important role in most cells. The function of each of these complexes is dependent on the
81 efficient assembly of up to 45 different proteins into a single complex (e.g. complex I, (20)).
82 The application of blue native polyacrylamide gel electrophoresis (BN-PAGE) allows these
83 complexes to be visualised. Not only critical to the production of cellular energy via
84 OXPHOS, mitochondria are also regulators of Ca^{2+} homeostasis, a source of reactive oxygen
85 species (ROS) production and act as a regulator of apoptotic signalling (4, 13). Mitochondrial
86 dysfunction has been suspected to be an important pathogenic feature in Duchenne
87 muscular dystrophy (18, 23). Potential mechanisms of this contribution could be a result of
88 the sustained increase in cytosolic Ca^{2+} in dystrophic muscle exerting a Ca^{2+} overload on the

89 mitochondrial transition pore which eventuates in apoptosis (8) and a consequent
90 decreased ability to produce ATP.

91 It has been suggested that mitochondria could be a therapeutic target for reducing the
92 severity of symptoms in DMD patients (30). Resting ATP content of dystrophic muscle was
93 reported to be ~50% of that seen in a healthy cohort (2, 6). This could be due to a
94 decreased ability to produce ATP, as analyses of isolated or enriched mitochondrial
95 preparations demonstrated a reduction in mitochondrial ATP production rate (MAPR) and
96 OXPHOS capacity in the *mdx* mouse (18, 30, 32). The decline in ATP could also be due to the
97 increased rate of ATP consumption, for such processes as driving the increased SERCA
98 activity necessary to try and maintain Ca²⁺ homeostasis and/or increased muscle
99 regeneration.

100 While not completely understood, it has further been suggested that the reduced
101 bioenergetic status presented by the reduced ATP in dystrophic muscle may be attributable
102 to morphologically compromised mitochondria, such as becoming swollen, which alters
103 mitochondrial function (23). Necessary for mitochondrial fusion, mitofusin 2 (Mfn2) is
104 responsible for the maintenance of healthy mitochondrial function, fusing together
105 damaged mitochondria that would otherwise contribute to excess ROS production and
106 subsequent muscle damage (33). Mfn2 was increased in the EDL and diaphragm of the
107 utrophin- dystrophin deficient mouse (29), although it is not known if this is altered in
108 muscle from the less severely affected *mdx* mouse. Whilst studies investigating
109 mitochondrial dynamics previously have examined different proteins involved in
110 mitochondrial fission, such as Fis1 and Opa1, these proteins are also involved in the fission
111 of other organelles, such as peroxisomes and so it is not possible to relate findings
112 specifically to mitochondria (21). Recently, mitochondrial dynamics protein 49 (MiD49) and
113 MiD51 were identified as mitochondrial specific proteins for fission, involved in recruiting
114 Drp1 to the outer mitochondrial membrane (31). MiD49 has only recently been described in
115 skeletal muscle (39) and whether it is altered in dystrophic muscle is not known.

116 Taurine is an amino acid found ubiquitously in all mammalian cells, and whilst not classified
117 as essential has extensively been characterised as vital for healthy muscle function and
118 development (9, 16). Dystrophin deficiency has been shown to impact taurine metabolism

119 (34). In the *mdx* mouse limb muscle taurine levels have been found to be reduced both
120 before and during the onset of severe dystropathology (21-28 d), before returning to
121 endogenous levels as the pathology stabilises into adulthood (70 d) (11, 22). The availability
122 of sufficient taurine both before and during these critical stages is therefore an area of
123 interest for the potential attenuation of the dystrophic pathology shown in the *mdx* mouse.
124 Taurine deficiency has been studied using a taurine transporter knockout mouse where
125 intramuscular taurine is almost absent (37). Such studies demonstrate pathological
126 symptoms indicative of those seen with dystrophin deficiency, indicating that taurine has a
127 role in mitochondrial function and energy production and may serve as a regulator of
128 mitochondrial protein synthesis, enhance the activity of the electron transport chain and
129 protect the mitochondria against excessive ROS generation (14, 15, 17). Of importance to
130 clinical outcomes, studies administering taurine via whole body supplementation or by
131 applying directly to muscle preparations have found it effective at improving muscle health
132 and/or force development (3, 7, 10, 35). Taurine deficiency has also been linked to cell
133 damage associated with increased oxidative stress (15, 17). One interesting point is that in
134 cardiomyocytes of rats depleted of taurine by beta-alanine, the activity of mitochondrial
135 complex I and III, and thus the electron transport chain, was suppressed (17). This was
136 supported by an apparent decrease in the abundance of complex I subunits ND5 and ND6,
137 albeit in fractionated samples which presents problems as the total mitochondrial pool was
138 not assessed (39).

139 To better understand the impact of disease severity and the potential of taurine as a
140 substance of therapeutic benefit to DMD we investigated markers of mitochondrial
141 content, activity and dynamics in the *mdx* mouse during both peak (28 d) and stable (70 d)
142 pathology, using the same mice we described in a recent paper (3). Using whole muscle
143 homogenates we investigated mitochondrial complexes in their native state by BN-PAGE,
144 complex sub-units NDUFA9 and COX IV as protein indicators of mitochondrial content,
145 citrate synthase (CS) as a measure of both mitochondrial content and activity, the
146 abundance of fusion and fission proteins, Mfn2 and MiD49, respectively, as markers of
147 mitochondrial dynamics and visualised mitochondrial distribution and abundance through
148 confocal immunohistochemistry.

149

150 **Materials & Methods**

151

152 ***Animals and supplementation.***

153 All procedures in this study were approved by the La Trobe University Animal Ethics
154 Committee (approval numbers 12-31, 13-48). Only male mice were used with n=35 *mdx* and
155 n=24 wild-type (WT, C57/BL10ScSn) animals in total. Experimental animals were bred at the
156 La Trobe Animal Research and Teaching Facility using breeding pairs obtained from the
157 Animal Resource Centre (Western Australia, Australia). The offspring of WT and *mdx* mice
158 had access to standard rat chow, water *ad libitum* and were utilised for experimentation at
159 either 28 ±1 or 70 ±1 days of age. Maximum litter size grown to maturity was 6 males. There
160 was no significant difference between body weights of each age group at the age of
161 experimentation (3). *Mdx* taurine (tau) breeders and subsequent offspring were
162 supplemented with continuous access to taurine (2.5% wt/vol) enriched drinking water,
163 with breeders beginning supplementation at least two weeks prior to mating. This dosage of
164 supplementation has been demonstrated previously to elevate skeletal muscle taurine
165 content in *mdx* mice (3).

166 ***Muscle dissection***

167 Mice were anaesthetised with an intraperitoneal injection of Nembutal (Sodium
168 Pentobarbitone) and kept unresponsive to tactile stimuli while the *extensor digitorum*
169 *longus* (EDL) and soleus muscles were excised, blotted clean on filter paper (Whatman No.1)
170 and weighed, before being snap frozen in liquid nitrogen. All muscles were stored at -80°C
171 until analysis. Mice were then killed by cardiac excision.

172

173 **Western Blotting**

174 Frozen transverse EDL and soleus cryosections were taken from the midpoint (~30 x 10 µm
175 28 d animals, ~20 x 10 µm 70 d animals) and immediately placed into a very low [Ca²⁺]
176 intracellular relaxing physiological buffer containing (in mM): 129 K⁺, 36 Na⁺, 1 free Mg²⁺
177 (10.3 total Mg²⁺), 90 HEPES, 50 EGTA, 8 ATP, 10 CP, pH 7.10, and an osmolality of 295 ±10
178 mosmol·kg·H₂O⁻¹). The sections were then diluted 2:1 with 3X SDS solution (0.125 M Tris-
179 HCl, 10% glycerol, 4% SDS, 4 M urea, 10% mercaptoethanol and 0.001% bromophenol blue,
180 pH 6.8) and kept at room temperature for a further 30 minutes, vortexed at five minute
181 intervals and stored at -80°C until analysed.

182 Aliquots of each EDL and soleus sample were pooled together and used to create a
183 calibration curve for that respective muscle that was run on every gel, allowing comparisons
184 of whole muscle homogenates across gels (25, 27). Total protein from each sample was
185 initially separated on 4-15% gradient Criterion TGX Stain Free gels (BioRad, Hercules, CA)
186 and following UV activation using a Stain Free Imager (BioRad), the densities of the total
187 lanes were obtained (Image lab software v 5.2, BioRad) and used to ensure equal loading for
188 subsequent western blotting.

189 Western blotting was performed to determine the protein abundance of mitochondrial
190 proteins COX IV, NDUFA9, Mfn2 and MiD49. The western blotting protocol was similar to
191 that described previously (26). Briefly, a similar amount of protein from skeletal muscle
192 samples was separated on 4-15% gradient Criterion TGX Stain Free gels (BioRad, Hercules,
193 CA). Prior to transfer gels were imaged with a Stain Free Imager (BioRad) for total protein
194 which was quantified for each sample using Image lab software (v 5.2, BioRad). Following
195 this, using a wet transfer protocol, protein was transferred onto a nitrocellulose membrane
196 at 100V for 30 min. Following transfer the gel was imaged again and the membrane
197 incubated in Pierce Miser solution (Pierce, Rockford, IL) for ~10 min and then blocked in 5%
198 skim milk powder in 1% Tris-buffered, saline-Tween (TBST) for ~2 h at room temperature.
199 Following blocking, membranes were incubated in primary antibodies overnight at 4°C and 2
200 h at room temperature. Antibody details and dilutions: cytochrome C oxidase subunit IV
201 (COX IV, rabbit polyclonal, 1:1000, #4844, Cell Signalling), NADH:ubiquinone
202 oxidoreductase subunit A9 (NDUFA9, rabbit polyclonal, 1:1000), Mfn2 (rabbit polyclonal,

203 1:500), MiD49 (rabbit polyclonal, 1:500, see (28, 31). *Mdx* mice were probed for dystrophin
204 (mouse monoclonal, 1:500, MANDYS1 clone 3B7, Development Studies Hybridoma Bank
205 (DSHB), Iowa, OH, USA) to confirm the absence of this protein. All antibodies were all
206 diluted in 1% bovine serum albumin (BSA) in phosphate buffered saline (PBS) with 0.025%
207 Tween (PBST).

208 After washing, membranes were incubated with a secondary antibody (goat anti-mouse IgG
209 or IgM, goat anti-rabbit IgG, HRP conjugated, 1:60,000) and rinsed in TBST. Bands were
210 visualized using West Femto chemiluminescent substrate (ThermoScientific, IL, USA) and
211 images taken and densitometry performed using Image Lab software (BioRad). The positions
212 of molecular mass markers were captured under white light, and then chemiluminescent
213 imaging was taken without moving the membrane. Total protein and specific protein
214 densities were each expressed relative to their respective calibration curves and
215 subsequently each protein was normalised to the total protein content (27). Data was then
216 expressed relative to the average of the 28 d WT on a given gel. Representative blots for
217 figures have been created by superimposing blots on top of the molecular mass marker,
218 with black lines indicating non congruent images from the same probe.

219

220 ***Citrate Synthase Activity Assay***

221 For determination of citrate synthase (CS) activity, muscle was accurately weighed (10-21
222 mg) and homogenised (5 x 5 s, with 5 min on ice between bursts) at 20:1 in buffer
223 containing 70 mM sucrose, 220 mM D-mannitol, 10 mM HEPES (pH 7.4), 1 mM EGTA.
224 Measurements were made in whole muscle preparations in duplicate or triplicate. Placed
225 into a reference cuvette was: 825 μL of 0.1 M Tris buffer, 100 μL of 5'-dithiobis (2-
226 nitrobenzoic acid) (DNTB, 0.5 $\text{mg}\cdot\text{mL}^{-1}$ made in Tris buffer) and 10 μL of acetyl-coA (6 $\text{mg}\cdot\text{mL}^{-1}$
227 1 made in Tris buffer). The cuvette was placed in a spectrophotometer (LKN Novaspec II,
228 Pharmacia Biotech, Sweden) and the machine was zeroed at 412 nm. Into individual
229 cuvettes containing the same components as the reference cuvette, 15 μL of homogenate
230 was added in addition to 50 μL of oxaloacetate (6.1 $\text{mg}\cdot\text{mL}^{-1}$ made in Tris buffer) to initiate
231 the reaction. Absorbance was recorded at 412nm every 15s for a total of 150 s. The change
232 in absorbance readings (Δ Abs) were plotted against time integrals (15 s) and linear

233 regression used to determine the slope of the response. The slope between 30 and 90 s
234 was used to calculate CS activity, which is presented as $\mu\text{mol}\cdot\text{min}^{-1}\cdot\text{g}^{-1}$.

235

236 ***Blue Native PAGE (BN-PAGE)***

237 To assess if mitochondrial complexes were present in their entirety we investigated
238 mitochondrial complexes utilising BN-PAGE. Samples were cryo-sectioned and placed in Na-
239 EGTA solution (described in whole muscle homogenate section) with 1% Triton-X100 (~30 x
240 10 μm 28 d animals, ~20 x 10 μm 70 d animals in 100 μL buffer). 10 μL of each sample were
241 diluted 1:1 in solubilising solution (20 mM Bis-Tris pH 7.0, 50 mM NaCl, 10% glycerol, 0.5%
242 Coomassie) with 2 μL of loading dye (5% Coomassie blue G, 500 mM ϵ -amino n-caproic acid,
243 100 mM Bis-Tris pH 7.0). Samples were loaded onto 4-13% native polyacrylamide gels
244 (Novex, Invitrogen). Gels were run for 10 min at 100V, 10 min at 400V and a 45 min at
245 400V, with a change of buffer between the second and third run. Following separation,
246 protein was transferred to PVDF membrane for 2 h at 100V. Membranes were stained
247 (Coomassie blue G, 50% methanol, 10% acetic acid), destained (50% methanol, 10% acetic
248 acid) and blocked for 2 h using 5% skim milk in TBST. Following blocking, the OXPHOS
249 antibody cocktail (Mouse, 1:1000, Abcam) was applied and methodology from here to
250 imaging is as described for Western blotting. Following imaging the remaining portions of
251 the samples were diluted 1:2 in 3x SDS loading buffer and run on a 4-15% Stain-Free
252 denaturing gel for the total protein used for quantification of each complex.

253

254 ***Immunohistochemistry (confocal microscopy)***

255 To visualise COX IV and identify mitochondria in tissue sections, transverse cryosections (8-
256 10 μm) were cut from the midpoint of the EDL and soleus muscles, and mounted on
257 positively charged microscope slides (Lomb Scientific). Cryosections were left at room
258 temperature for ~10 min, then the fixative (4% paraformaldehyde in PBS; PFA) added for 30
259 min. Afterwards, cryosections were washed (3 x 10 min in PBS), followed by immunobuffer
260 (50 mM glycine, 0.033% saponin, 0.25% BSA, 0.05% sodium azide) and incubation for 2
261 hours. COX IV antibody (1:100, same source as western blotting), diluted in immunobuffer

262 was added and sections incubated overnight at room temperature in an airtight, saturated
263 container. Sections were washed with immunobuffer (3 x 10 min), before secondary
264 antibody (1:2000 in immunobuffer, Donkey anti-rabbit Alexis 488 (Abcam, ab150061)) was
265 added and sections incubated for 2 hours at room temperature. Sections were then washed
266 in immunobuffer (10 min) before adding DAPI (1:1000 in immunobuffer, 2 min) for
267 visualizing nuclei. A negative control slide was obtained by following the above steps with
268 the omission of primary antibody, where immunobuffer was used during that incubation
269 step. Sections were finally washed (2 x 10 min, PBS) before being air-dried, and a coverslip
270 carefully applied with a drop of ProLong Diamond Antifade Mountant (Thermo Fisher,
271 P36961), and the coverslip sealed with nail polish. Fluorescently labelled samples were
272 stored in the dark at -20°C. Images were all taken at the same magnification with a Zeiss
273 780 confocal laser-scanning microscope (Zeiss AxioObserver Z1, Carl Zeiss Microscopy,
274 Oberkochen, Germany).

275

276 ***Statistics***

277 All data are presented as mean \pm standard deviation (SD). Comparisons between relevant
278 groups was performed using a One-way ANOVA of variance, with Holm-Sidak's post-hoc
279 analyses. All statistical analysis was performed using GraphPad Prism v 6. Significance was
280 set at $p < 0.05$.

281

282 **Results**

283 **Mitochondrial complex I, II, IV and V abundances**

284 The abundance of mitochondrial complexes were assessed using BN-PAGE with duplicate
285 measurements of each sample. No difference in the abundances or the apparent migrations
286 of complexes I, II, IV or V were found in the soleus muscle of WT, *mdx* and *mdx* Tau mice (Fig
287 1).

288 **NDUFA9 and COX IV protein.**

289 In soleus muscle the mitochondrial marker associated with complex I, NDUFA9, was
290 decreased by approximately 50% in *mdx* mice at both 28 and 70 d compared to age
291 matched WT mice (Fig 1A). 70 d *mdx* tau mice exhibited an approximate 50% increase in
292 NDUFA9 protein abundance when compared to the *mdx* group, this increase was not
293 observed between 28 d *mdx* and *mdx* tau supplemented mice (Fig 2A). NDUFA9 abundance
294 was elevated significantly with age in both the WT and *mdx* groups (Fig 2A). EDL NDUFA9
295 protein abundance was reduced in 28 d *mdx* mice when compared to the WT, with no
296 further differences observed with NDUFA9 protein abundance between groups (Fig 2B).
297 There was no differences in soleus or EDL COX IV protein abundances between any groups
298 (Fig 2C-D).

299 **Citrate synthase activity.**

300 The enzyme citrate synthase is a validated biomarker for mitochondrial density in skeletal muscle,
301 and CS activity is widely used as measure of oxidative capacity (19) and thereby was used in the
302 current study. There was an age specific effect on soleus CS activity, with 70 d old WT, *mdx*
303 and *mdx* tau mice all exhibiting more than two-fold increase relative to the 28 d animals
304 from the same group (Fig 3A). There were no group specific differences in EDL CS activity at
305 either 28 or 70 d (Fig 3B). There was approximately 20% less CS activity in 28 d *mdx*
306 compared with WT mice, with no further differences observed between groups or ages (Fig
307 3B).

308

309

310 **Mitochondrial dynamics, Mfn2 and MiD49, proteins.**

311 There were no differences observed in the abundance of Mfn2 and MiD49 proteins in either
312 soleus or EDL muscles in any group (Fig 4).

313 **Immunohistochemistry**

314 Mitochondrial abundance following immunostaining was visualised using confocal
315 microscopy. Staining of muscle sections with COX IV antibody revealed a qualitatively
316 similar abundance of mitochondria across all treatment types (Fig. 5), as observed by
317 western blot analysis (Fig. 2). There was no discernible difference in staining intensity
318 between the EDL and soleus muscles of 28 d mice, but there was heterogeneity of COX IV
319 staining intensity observed between muscle fibres. Presumably greater COX IV, and
320 therefore mitochondria, is present in the slow twitch oxidative fibres while a lesser intensity
321 is presented in the more glycolytic fast twitch fibers.

322 DAPI stain revealed a higher abundance of centralised myonuclei and infiltration of other
323 nuclei in both EDL and soleus muscles of 28 d *mdx* mice, which were present to a lesser
324 extent in *mdx* tau treated and WT mice (Fig. 5). This trend was not observed in the soleus
325 muscle of 70 d mice (Fig. 5).

326 **Discussion**

327 The current study provides muscle specific insights into the effect of age on mitochondria in
328 wild-type and the *mdx* mouse model of DMD. It also addresses whether the benefits of
329 taurine supplementation on muscle function (3) are due to changes in mitochondrial
330 content or activity.

331 We investigated the abundance of whole mitochondrial respiratory complexes I, II, IV and V
332 in their native state by BN-PAGE and found no differences in the abundances or the relative
333 migration of these complexes between WT and *mdx* mice in either 28 d animals, when the
334 dystrophic phenotype would be active and the most damage occurring, or during stable
335 stages of muscle damage at 70 d (Fig 1B). The examination of mitochondrial complexes by
336 BN-PAGE has the advantage of providing information about not only complex abundance
337 but the formation of individual complexes. Each complex consists of numerous individual
338 proteins, e.g. complex I has 45 subunits and migrates at ~1,000 kDa when containing its full
339 complement of protein subunits (38). These data suggest that at least the majority of the
340 subunits assembled for a given complex, are similar between phenotype and ages.

341 Given that no differences were seen in mitochondrial complexes, we then went on to
342 examine two important markers of mitochondrial complex abundance by western blotting
343 using calibration curves and small sample amounts, which provide the most quantitative
344 approach (27). The protein NDUFA9 is one of the 45 subunits that comprise mammalian
345 complex I (24) and has been used previously as a marker of both complex abundance and
346 total mitochondrial content (39). Interestingly, there was ~two-fold less NDUFA9 protein in
347 soleus muscle from *mdx* mice at both 28 and 70 d compared with WT mice (Fig 2A). In EDL
348 muscle this was only seen in 70 d animals (Fig 2B). In soleus muscles from both WT and *mdx*
349 mice there was ~two-fold increase in NDUFA9 abundances with age (Fig 2A). Given that
350 NDUFA9 is an ~36 kDa protein, then on its own, it would not be expected to be observed as
351 a difference in the migration or the abundance of the total Complex I on BN-PAGE. Whilst
352 NDUFA9 is part of Complex I, it is unclear if a change in its abundance would affect overall
353 mitochondrial function (24). However the decrease in NDUFA9 protein abundance found
354 here does coincide with reports of a deficiency in Complex I function that was apparent in
355 muscle from *mdx* compared with WT animals (32). It was pleasing that the mitochondrial

356 yields were reported in that paper and worth due consideration was the low mitochondrial
357 yields (10-18%) and a difference in the yields between muscle from *mdx* and WT mice (32).
358 Interestingly, in cardiac muscle from *mdx* mice cardiomyocytes have been shown to exhibit
359 altered mitochondrial activity that was not evident at the level of isolated mitochondria,
360 suggesting the problem exists on a cellular as opposed to organelle level (36). Such studies
361 highlight the importance of investigating mitochondrial function in the context of its role
362 within the cell as well as in isolation. An important and novel aspect of our study is the use
363 of whole muscle for all our biochemical analyses including BN-PAGE, western blotting and
364 CS activity. Studies undertaking mitochondrial research involving centrifugation of tissue
365 samples may be underestimating mitochondrial content, as recently Wyckelsma et al. (39)
366 identified approximately 10-40% of mitochondria are discarded and, very importantly, the
367 yields were different when measuring different mitochondrial proteins and different
368 samples were used. A further and more detailed description of the issues associated with
369 quantitative assessment following fractionation of tissue are reported by Murphy and Lamb
370 (27).

371 Our second protein marker of mitochondrial abundance was COX IV, has been established
372 as being essential for complex IV (Cytochrome-c oxidase) function (20). We found no
373 difference in the protein abundance of COX IV between *mdx* and WT groups in both soleus
374 and EDL muscle at both ages (Fig 2D). This, in combination with BN-PAGE data, suggests that
375 Complex IV is not altered in dystrophic muscle, or as a consequence of age. Qualitative
376 visualisation of COX IV through confocal microscopy further confirmed these results,
377 revealing no appreciable difference between muscle types, age and tau treatment (Fig 5).
378 There was however a fibre specific heterogeneity in the intensity of COX IV, with greater
379 intensity observed in presumably type I slow twitch oxidative fibres as opposed to glycolytic
380 type II fibres (Fig 5).

381 Shown to be strongly associated with mitochondrial content and the ability of the
382 mitochondria to produce ATP (oxidative capacity) (19), we also investigated CS activity in
383 muscles from the *mdx* and WT animals at both ages. We found no change in CS activity
384 when comparing soleus muscle from *mdx* and WT mice, either at 28 or 70 d (Fig 3A). When
385 the effect of age was examined in soleus muscles, CS activity was increased ~two-fold in

386 both *mdx* and WT mice 70 d mice compared to their respective 28 d mice (Fig 3).
387 Interestingly this age specific increase was of similar magnitude to that observed in NDUFA9
388 protein abundance (Fig 2A). Whilst it is tempting to speculate that the NDUFA9 protein
389 abundance is either responding to or driving the age dependent increase in oxidative
390 capacity of Complex I in soleus muscle, it cannot explain the decreased NDUFA9 protein
391 abundance seen in soleus muscle of *mdx* compared with WT mice. It is clear that further
392 studies are required to elucidate the reason behind the age related changes in CS activity.

393 This is the first work to investigate the abundance of the mitochondrial specific dynamics
394 proteins, Mfn2 and MiD49, in whole skeletal muscle from the *mdx* mouse. There were no
395 differences in protein abundances of either Mfn2 or MiD49 across both soleus and EDL
396 muscles and across groups (Fig 4). Based on the previously published suggestion that total
397 oxidative capacity (measured as MAPR and OXPHOS) may be reduced in *mdx* mice, we had
398 thought mitochondrial dynamics would be increased. It was surprising, therefore, to see
399 that there was no evidence of altered abundance in Mfn2 or MiD49 in the *mdx* mouse
400 during 28 d where the period where peak muscular damage occurs and muscle turnover is
401 high. Interestingly, a recent study reported a several-fold increase in the abundance of Mfn2
402 in the EDL muscle of 8 week old utrophin-dystrophin deficient mouse (29). The utrophin-
403 dystrophin deficient mouse model cannot be directly compared with the less severe *mdx*
404 mouse model because it experiences a more severe phenotype of muscle damage. Those
405 data provide evidence, however, that Mfn2 can be upregulated in a compensatory capacity
406 in response to either increased mitochondrial damage or energy demand that was not seen
407 in the present study. That study also found an increase in Drp1 (29), although given that
408 Drp1 is involved with the fission of peroxisomes as well as mitochondria, it limits the
409 interpretation of that finding in relation specifically to mitochondria. We have recently
410 reported both Mfn2 and MiD49 to be increased in muscle from aged compared with young
411 adults, further supporting the dynamic response of these proteins (39).

412 Previously we identified that taurine supplementation was effective at increasing strength
413 and improving the histological profile of the *tibialis anterior* muscle in *mdx* mice during the
414 peak damage period of 28 d utilising the same mice and treatment regime as the present
415 study (3). In the current study we investigated whether the beneficial effects of taurine

416 were associated with an increase in markers of oxidative capacity or mitochondrial
417 abundance. Visualisation of nuclei using fluorescent DAPI staining revealed taurine to have a
418 seemingly beneficial effect on the visible health of EDL and soleus muscles of 28 d *mdx*
419 taurine treated mice, as seen with hematoxylin and eosin staining (3). However, while an
420 increase in NDUFA9 protein abundance was observed in the 70 d *mdx* tau mouse when
421 compared to the non-supplemented *mdx* mouse there was no effect of taurine on any other
422 measure of mitochondrial content or activity. While our current data suggests that taurine
423 affords no mitochondrial adaptation in the *mdx* mouse at either 28 or 70 d of age, it remains
424 that complex I activity can be selectively impaired without detectable changes in complex
425 content or mitochondrial volume/density. Subsequently a possible mechanism for
426 functional improvement with taurine supplementation could be a reduction in the
427 impairment of electron transport secondary to an antioxidant effect at complex I (17). It is
428 thereby not wholly conclusive in the current study that taurine supplementation did not
429 elicit some mitochondrial adaptation which requires further investigation. Future studies
430 should assess mitochondrial function *in situ* and include high-resolution respirometry, while
431 ultrastructural mitochondrial reticular comparison would be of interest to support or refute
432 the relevance of absolute measures of Mfn2 and MiD49 for mitochondrial dynamics.

433 **Conclusion**

434 Our assessment of mitochondria using an array of approaches (BN-PAGE, western blotting,
435 confocal microscopy and CS activity) suggest there is no reason to believe that
436 mitochondrial content is reduced in *mdx* mouse, at either 28 d when peak damage is
437 occurring, or at 70 d when the muscle is stabilised. In order to further elucidate this, there is
438 an absolute need for future functional mitochondria assays to be undertaken in whole
439 muscle preparations, where the entire mitochondrial pool are represented.

440 **Acknowledgements**

441 We would like to acknowledge Dr. Peter Lock and the LIMS BioImaging facility for assistance
442 with obtaining the confocal images used in the present study.

443

444

445 **Figure Legends**

446 **Figure 1. Native state complex abundance in soleus muscle of 28 and 70 d WT, *mdx* and**
447 ***mdx tau* mice. (A)** Myosin from the Stain Free gel, indicative of total protein (*top*),
448 Representative blot of Blue Native PAGE using OXPHOS cocktail antibody (*bottom*). **(B)**
449 Complex I, II, IV and V abundances normalised to the average of the 28 d WT from 28 d
450 (solid symbols) and 70 d (open symbols) WT (circles), *mdx* (triangles) and *mdx tau* (squares)
451 mice. One way ANOVA with Holm-Sidak's post-hoc analyses between relevant groups. Data
452 presented as data points surrounding means \pm SD, n indicated by number of symbols.

453 **Figure 2. Mitochondrial protein abundance in soleus and EDL muscles of 28 and 70 d WT,**
454 ***mdx* and *mdx tau* mice.** Shown for each panel is the myosin from the Stain Free gel,
455 indicative of total protein (*top*), the representative Western blot protein (*middle*), and
456 quantification of protein abundance (*bottom*) from 28 d (solid symbols) and 70 d (open
457 symbols) WT (circles), *mdx* (triangles) and *mdx tau* (squares) mice. NDUFA9 in soleus **(A)** and
458 EDL **(B)** and COX IV in soleus **(C)** and EDL **(D)**, each expressed relative to the 28 d WT. One
459 way ANOVA with Holm-Sidak's post-hoc analyses between relevant groups. Data presented
460 as data points surrounding means \pm SD, n indicated by number of symbols. Lines connecting
461 different bars indicate significance at $p < 0.05$, *** $p < 0.001$.

462 **Figure 3. Citrate synthase activity in soleus and EDL muscles of 28 d compared 70 d wild-**
463 **type, *mdx* and *mdx taurine (mdx tau)* mice. (A)** Soleus citrate synthase activity **(B)** EDL
464 citrate synthase activity assay from 28 d (solid symbols) and 70 d (open symbols) WT
465 (circles), *mdx* (triangles) and *mdx tau* (squares) mice. One way ANOVA with Holm-Sidak's
466 post-hoc analyses between relevant groups. Data presented as data points surrounding
467 means \pm SD, n indicated by number of symbols. Lines connecting different bars indicate
468 significance at * $p < 0.05$, *** $p < 0.001$.

469

470

471

472

473

474 **Figure 4. Mitochondrial dynamics protein abundance in soleus and EDL muscles of 28 and**
475 **70 d WT, *mdx* and *mdx* tau mice.** Shown for each panel is the myosin from the Stain Free
476 gel, indicative of total protein (*top*), the representative Western blot protein (*middle*), and
477 quantification of protein abundance (*bottom*) from 28 d (solid symbols) and 70 d (open
478 symbols) WT (circles), *mdx* (triangles) and *mdx* tau (squares) mice. **(A)** Fa9, **(B)** COX IV, **(C)**
479 Mfn2 and **(D)** MiD49 expressed relative to the 28 d WT. One way ANOVA with Holm-Sidak's
480 post-hoc analyses between relevant groups. Data presented as data points surrounding
481 means \pm SD, n indicated by number of symbols. Lines connecting different bars indicate
482 significance at $p < 0.05$.

483

484 **Figure 5. Confocal microscopy imaging of mitochondria and nuclei in 28 d and 70 d wild-**
485 **type, *mdx* and *mdx* taurine mice.** Transverse sections of EDL and soleus muscles from 28
486 and 70 d WT, *mdx* and *mdx* tau mice shown at 400 X magnification by confocal laser
487 scanning microscope. Nuclei are stained blue (DAPI), mitochondria are stained green (COX
488 IV protein). Greater intensity of color equates to greater abundance of COX IV. Fiber
489 outlines are evident. Scale bars = 100 μ m. Experiments repeated on n = 4 animals for all
490 groups.

491

492 **References**

493

- 494 1. **Allen DG, Whitehead NP, and Froehner SC.** Absence of Dystrophin Disrupts Skeletal Muscle
495 Signaling: Roles of Ca²⁺, Reactive Oxygen Species, and Nitric Oxide in the Development of Muscular
496 Dystrophy. *Physiol Rev* 96: 253-305, 2016.
- 497 2. **Austin L, de Niese M, McGregor A, Arthur H, Gurusinge A, and Gould MK.** Potential
498 oxyradical damage and energy status in individual muscle fibres from degenerating muscle diseases.
499 *Neuromuscular Disorders* 2: 27-33, 1992.
- 500 3. **Barker RG, Horvath D, van der Poel C, and Murphy RM.** Benefits of Pre-natal Taurine
501 Supplementation in Preventing the Onset of Acute Damage in the Mdx Mouse. *PLOS Currents*
502 *Muscular Dystrophy* 2017 doi: 10.1371/currents.md.9a3e357a0154d01050b591601cbd4fdb.
- 503 4. **Brookes PS, Yoon Y, Robotham JL, Anders MW, and Sheu SS.** Calcium, ATP, and ROS: a
504 mitochondrial love-hate triangle. *Am J Physiol Cell Physiol* 287: C817-833, 2004.
- 505 5. **Bushby K, Finkel R, Birnkrant DJ, Case LE, Clemens PR, Cripe L, Kaul A, Kinnett K, McDonald
506 C, Pandya S, Poysky J, Shapiro F, Tomezsko J, and Constantin C.** Diagnosis and management of
507 Duchenne muscular dystrophy, part 1: diagnosis, and pharmacological and psychosocial
508 management. *Lancet Neurology* 9: 77-93, 2010.
- 509 6. **Cole MA, Rafael JA, Taylor DJ, Lodi R, Davies KE, and Styles P.** A quantitative study of
510 bioenergetics in skeletal muscle lacking utrophin and dystrophin. *Neuromuscular disorders* 12: 247-
511 257, 2002.
- 512 7. **Cozzoli A, Rolland JF, Capogrosso RF, Sblendorio VT, Longo V, Simonetti S, Nico B, and De
513 Luca A.** Evaluation of potential synergistic action of a combined treatment with alpha-methyl-
514 prednisolone and taurine on the mdx mouse model of Duchenne muscular dystrophy.
515 *Neuropathology and Applied Neurobiology* 37: 243-256, 2011.
- 516 8. **Crompton M.** The mitochondrial permeability transition pore and its role in cell death.
517 *Biochem J* 341: 233-249, 1999.
- 518 9. **De Luca A, Pierno S, and Camerino DC.** Taurine: the appeal of a safe amino acid for skeletal
519 muscle disorders. *Journal of translational medicine* 13: 243, 2015.
- 520 10. **De Luca A, Pierno S, Liantonio A, Cetrone M, Camerino C, Fraysse B, Mirabella M, Servidei
521 S, Rungg UT, and Conte Camerino D.** Enhanced dystrophic progression in mdx mice by exercise and
522 beneficial effects of taurine and insulin-like growth factor-1. *J Pharmacol Exp Ther* 304: 453-463,
523 2003.
- 524 11. **Griffin JL, Williams HJ, Sang E, Clarke K, Rae C, and Nicholson JK.** Metabolic Profiling of
525 Genetic Disorders: A Multitissue 1H Nuclear Magnetic Resonance Spectroscopic and Pattern
526 Recognition Study into Dystrophic Tissue. *Analytical biochemistry* 293: 16-21, 2001.
- 527 12. **Grounds MD, Radley HG, Lynch GS, Nagaraju K, and De Luca A.** Towards developing
528 standard operating procedures for pre-clinical testing in the mdx mouse model of Duchenne
529 muscular dystrophy. *Neurobiol Disease* 31: 1-19, 2008.
- 530 13. **Gunter TE, Yule DI, Gunter KK, Eliseev RA, and Salter JD.** Calcium and mitochondria. *FEBS
531 Lett* 567: 96-102, 2004.
- 532 14. **Hansen SH, Andersen ML, Birkedal H, Cornett C, and Wibrand F.** The important role of
533 taurine in oxidative metabolism. *Adv Exp Med Biol* 583: 129-135, 2006.
- 534 15. **Hansen SH, Andersen ML, Cornett C, Gradinaru R, and Grunnet N.** A role for taurine in
535 mitochondrial function. *J Biomedical Science* 17 Suppl 1: S23, 2010.
- 536 16. **Huxtable RJ.** Physiological actions of taurine. *Physiological reviews* 72: 101-163, 1992.
- 537 17. **Jong CJ, Azuma J, and Schaffer S.** Mechanism underlying the antioxidant activity of taurine:
538 prevention of mitochondrial oxidant production. *Amino Acids* 42: 2223-2232, 2012.
- 539 18. **Kuznetsov AV, Winkler K, Wiedemann F, von Bossanyi P, Dietzmann K, and Kunz WS.**
540 Impaired mitochondrial oxidative phosphorylation in skeletal muscle of the dystrophin-deficient mdx
541 mouse. *Mol Cell Biochem* 183: 87-96, 1998.

- 542 19. **Larsen S, Nielsen J, Hansen CN, Nielsen LB, Wibrand F, Stride N, Schroder HD, Boushel R,**
543 **Helge JW, Dela F, and Hey-Mogensen M.** Biomarkers of mitochondrial content in skeletal muscle of
544 healthy young human subjects. *J Physiol* 590: 3349-3360, 2012.
- 545 20. **Li Y, Park J-S, Deng J-H, and Bai Y.** Cytochrome c oxidase subunit IV is essential for assembly
546 and respiratory function of the enzyme complex. *J Bioenergetics Biomembranes* 38: 283-291, 2006.
- 547 21. **Loson OC, Song Z, Chen H, and Chan DC.** Fis1, Mff, MiD49, and MiD51 mediate Drp1
548 recruitment in mitochondrial fission. *Mol Biol Cell* 24: 659-667, 2013.
- 549 22. **McIntosh L, Granberg KE, Briere KM, and Anderson JE.** Nuclear magnetic resonance
550 spectroscopy study of muscle growth, mdx dystrophy and glucocorticoid treatments: correlation
551 with repair. *NMR Biomedicine* 11: 1-10, 1998.
- 552 23. **Millay DP, Sargent MA, Osinska H, Baines CP, Barton ER, Vuagniaux G, Sweeney HL,**
553 **Robbins J, and Molkentin JD.** Genetic and pharmacologic inhibition of mitochondrial-dependent
554 necrosis attenuates muscular dystrophy. *Nature Med* 14: 442-447, 2008.
- 555 24. **Mimaki M, Wang X, McKenzie M, Thorburn DR, and Ryan MT.** Understanding mitochondrial
556 complex I assembly in health and disease. *Biochimica et Biophysica Acta (BBA) - Bioenergetics* 1817:
557 851-862, 2012.
- 558 25. **Mollica JP, Oakhill JS, Lamb GD, and Murphy RM.** Are genuine changes in protein
559 expression being overlooked? Reassessing Western blotting. *Anal Biochem* 386: 270-275, 2009.
- 560 26. **Murphy RM.** Enhanced technique to measure proteins in single segments of human skeletal
561 muscle fibers: fiber-type dependence of AMPK-alpha1 and -beta1. *J Appl Physiol (1985)* 110: 820-
562 825, 2011.
- 563 27. **Murphy RM, and Lamb GD.** Important considerations for protein analyses using antibody
564 based techniques: down-sizing Western blotting up-sizes outcomes. *J Physiol* 591: 5823-5831, 2013.
- 565 28. **Osellame LD, Singh AP, Stroud DA, Palmer CS, Stojanovski D, Ramachandran R, and Ryan**
566 **MT.** Cooperative and independent roles of the Drp1 adaptors Mff, MiD49 and MiD51 in
567 mitochondrial fission. *J Cell Sci* 129: 2170-2181, 2016.
- 568 29. **Pant M, Sopariwala DH, Bal NC, Lowe J, Delfin DA, Rafael-Fortney J, and Periasamy M.**
569 Metabolic dysfunction and altered mitochondrial dynamics in the utrophin-dystrophin deficient
570 mouse model of duchenne muscular dystrophy. *PLoS One* 10: e0123875, 2015.
- 571 30. **Percival JM, Siegel MP, Knowels G, and Marcinek DJ.** Defects in mitochondrial localization
572 and ATP synthesis in the mdx mouse model of Duchenne muscular dystrophy are not alleviated by
573 PDE5 inhibition. *Human Mol Genetics* 22: 153-167, 2013.
- 574 31. **Richter V, Palmer CS, Osellame LD, Singh AP, Elgass K, Stroud DA, Sesaki H, Kvensakul M,**
575 **and Ryan MT.** Structural and functional analysis of MiD51, a dynamin receptor required for
576 mitochondrial fission. *J Cell Biol* 204: 477-486, 2014.
- 577 32. **Rybalka E, Timpani CA, Cooke MB, Williams AD, and Hayes A.** Defects in mitochondrial ATP
578 synthesis in dystrophin-deficient mdx skeletal muscles may be caused by complex I insufficiency.
579 *PLoS One* 9: e115763, 2014.
- 580 33. **Sebastian D, Sorianello E, Segales J, Irazoki A, Ruiz-Bonilla V, Sala D, Planet E, Berenguer-**
581 **Llargo A, Munoz JP, Sanchez-Feutrie M, Plana N, Hernandez-Alvarez MI, Serrano AL, Palacin M, and**
582 **Zorzano A.** Mfn2 deficiency links age-related sarcopenia and impaired autophagy to activation of an
583 adaptive mitophagy pathway. *EMBO J* 35: 1677-1693, 2016.
- 584 34. **Terrill JR, Grounds MD, and Arthur PG.** Taurine deficiency, synthesis and transport in the
585 mdx mouse model for Duchenne Muscular Dystrophy. *Int J Biochem; Cell Biology* 66: 141-148, 2015.
- 586 35. **Terrill JR, Pinniger GJ, Graves JA, Grounds MD, and Arthur PG.** Increasing taurine intake and
587 taurine synthesis improves skeletal muscle function in the mdx mouse model for Duchenne muscular
588 dystrophy. *J Physiol* 594: 3095-3110, 2016.
- 589 36. **Viola HM, Davies SM, Filipovska A, and Hool LC.** L-type Ca(2+) channel contributes to
590 alterations in mitochondrial calcium handling in the mdx ventricular myocyte. *Am J Physiol Heart Circ*
591 *Physiol* 304: H767-775, 2013.

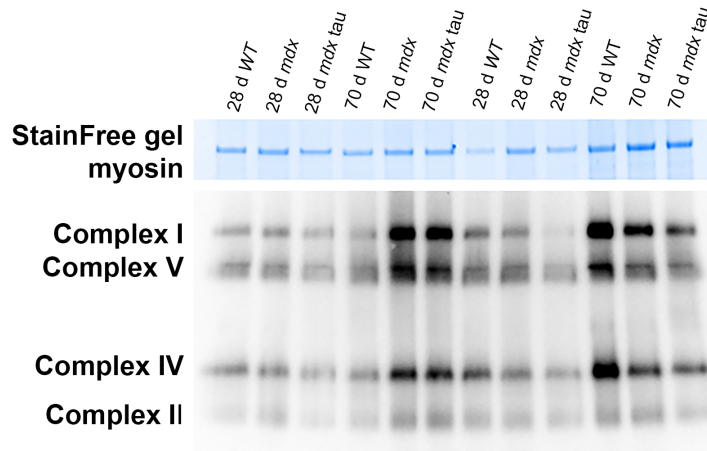
- 592 37. **Warskulat U, Flögel U, Jacoby C, Hartwig H, Thewissen M, Merx MW, Molojavyi A, Heller-**
593 **Stilb B, Schrader J, and Häussinger D.** Taurine transporter knockout depletes muscle taurine levels
594 and results in severe skeletal muscle impairment but leaves cardiac function uncompromised.
595 *FASEB J* 18: 577-579, 2004.
- 596 38. **Wittig I, Braun H-P, and Schagger H.** Blue native PAGE. *Nature Protocols* 1: 418, 2006.
- 597 39. **Wyckelsma VL, Levinger I, McKenna MJ, Formosa LE, Ryan MT, Petersen AC, Anderson MJ,**
598 **and Murphy RM.** Preservation of skeletal muscle mitochondrial content in older adults:relationship
599 between mitochondria, fibre-type & high intensity exercise training. *J Physiol* 595(11):3345-3359
600 2017.

601

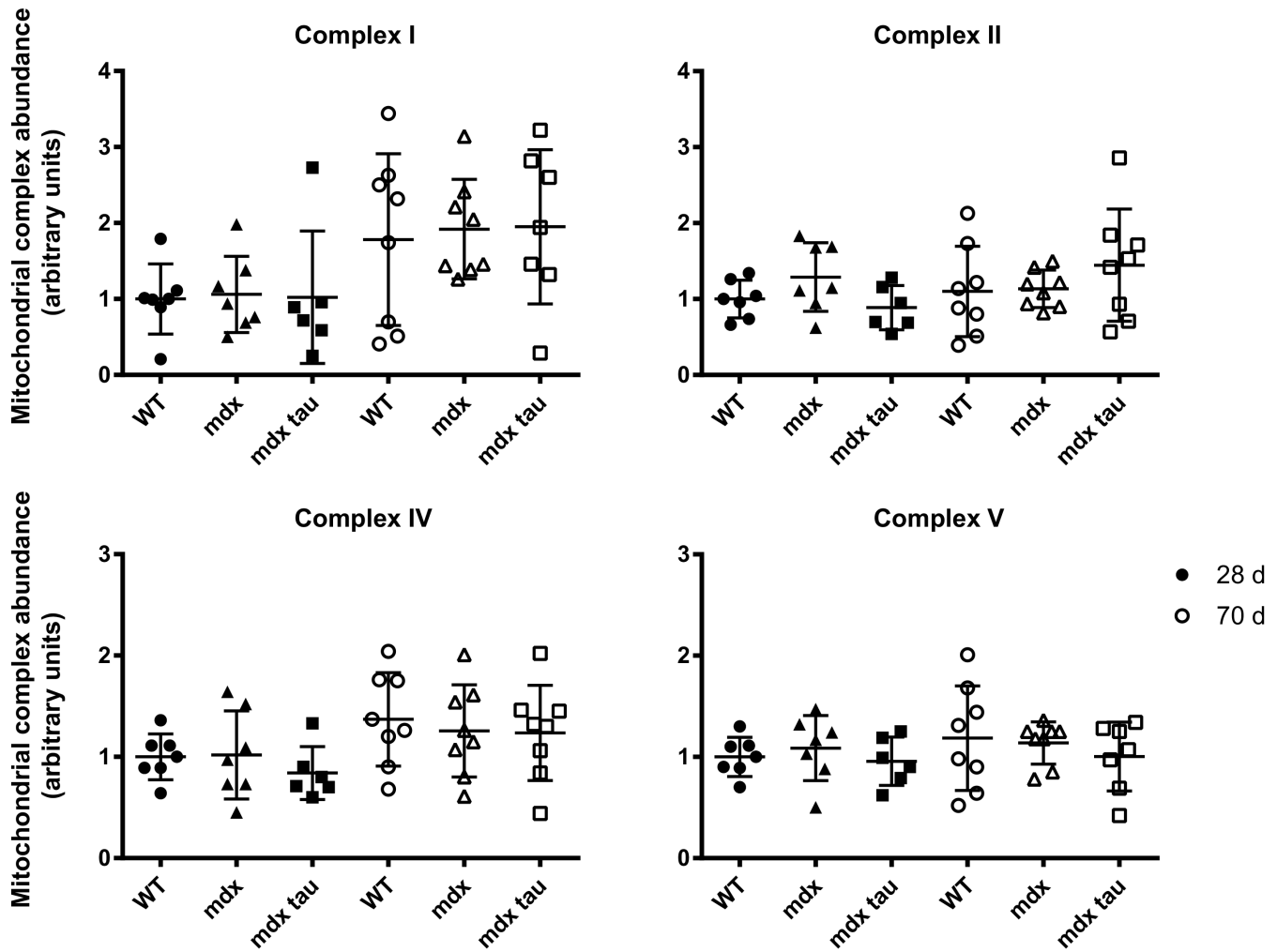
602

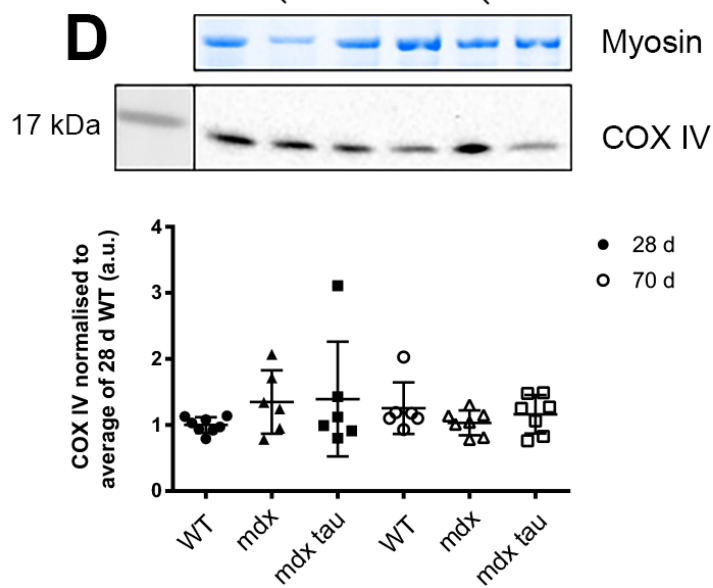
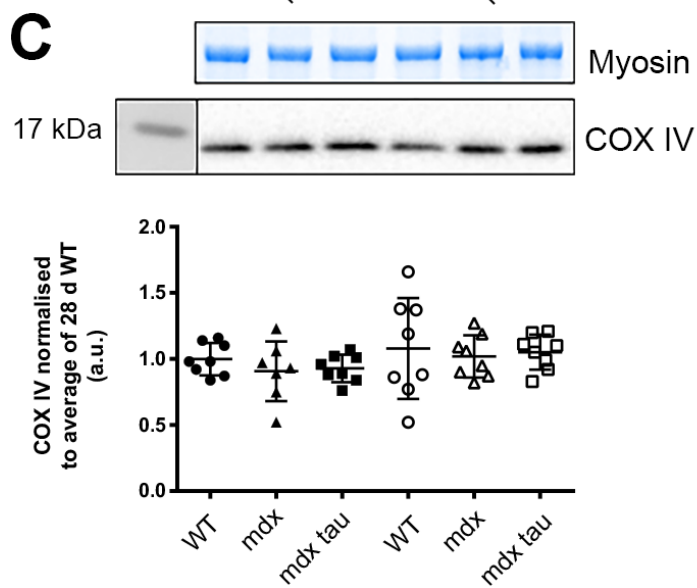
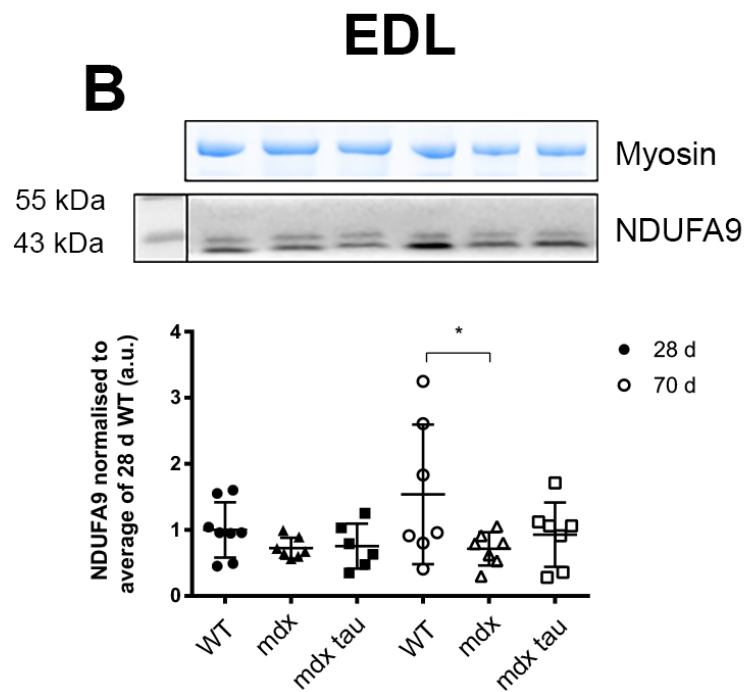
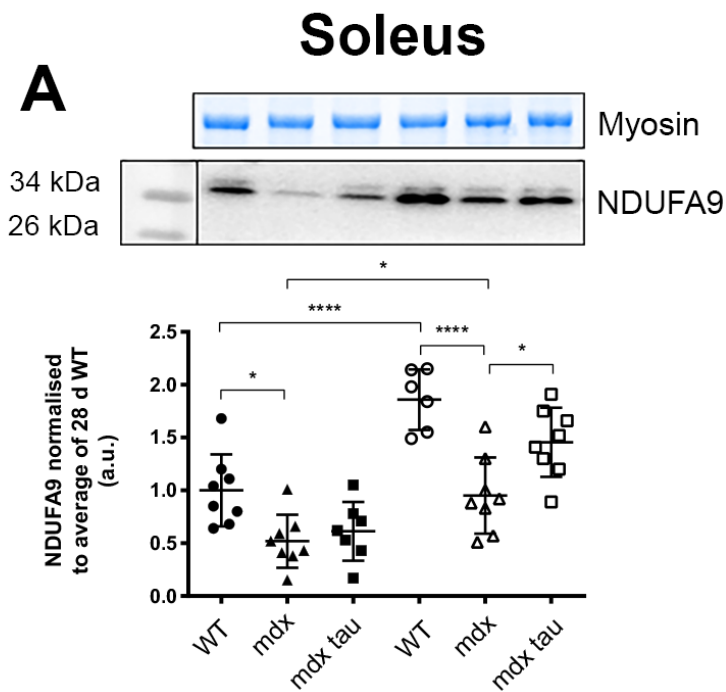
603

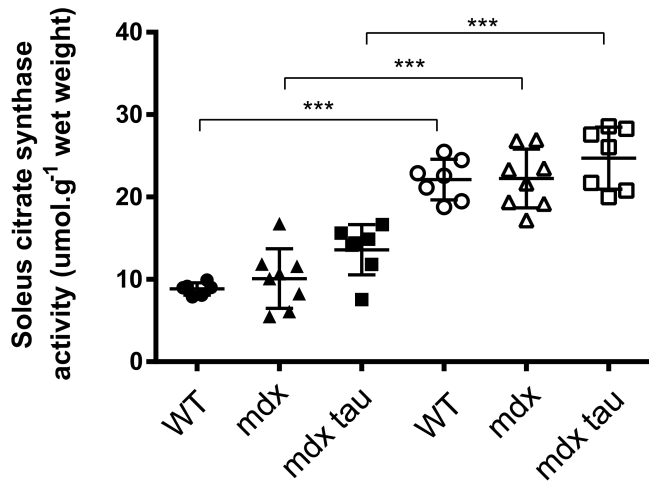
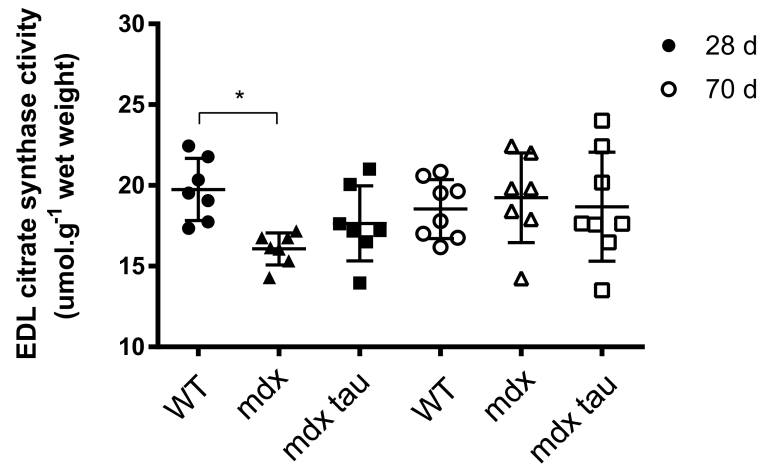
A



B

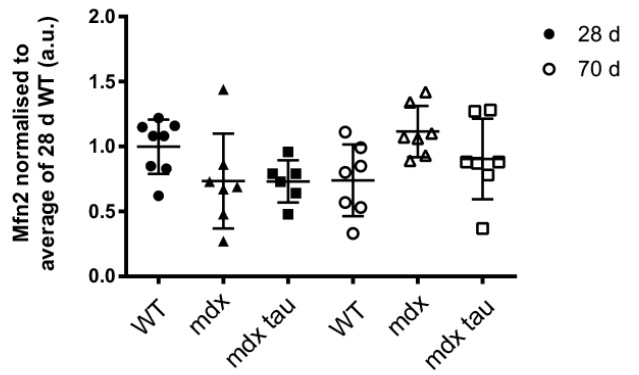
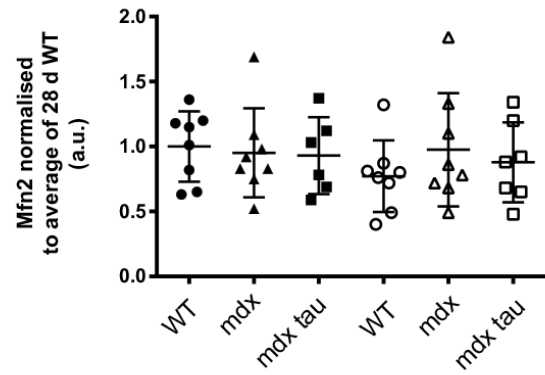
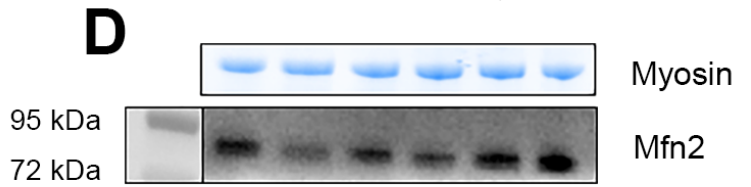
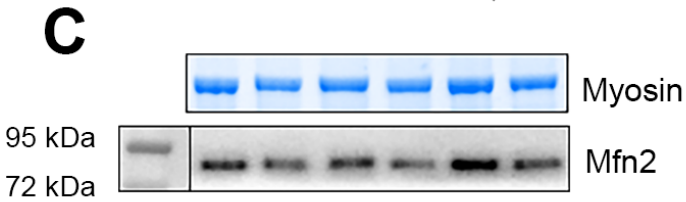
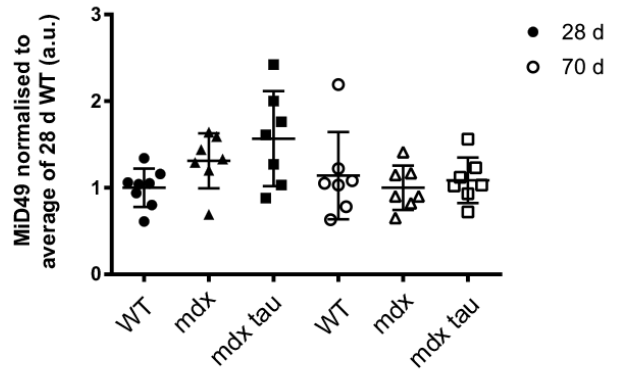
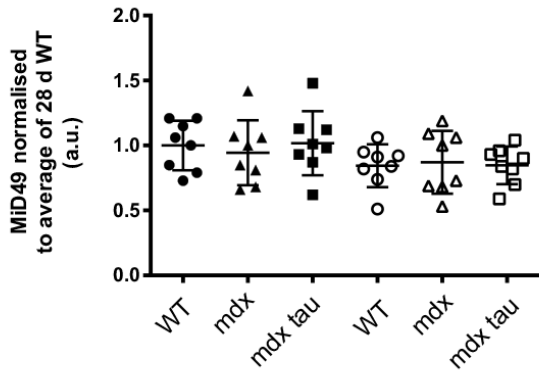
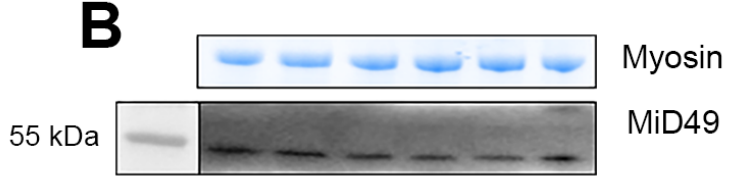
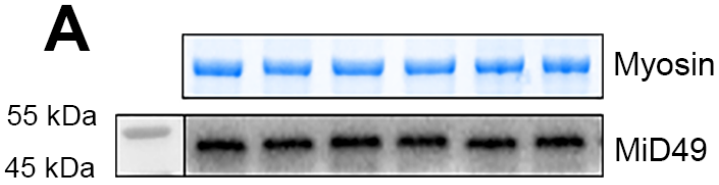




A**B**

Soleus

EDL

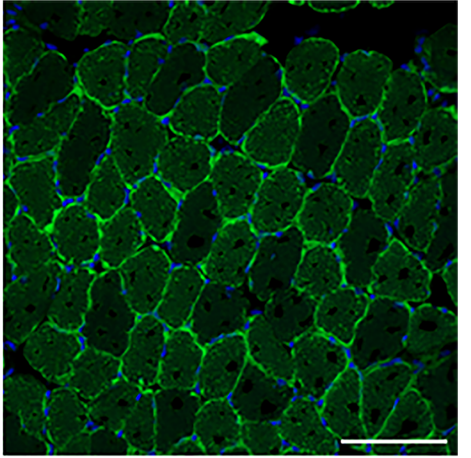
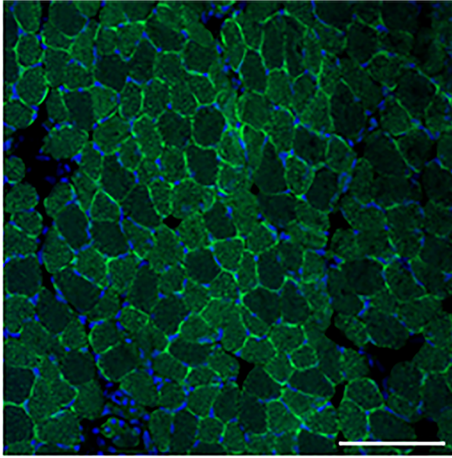
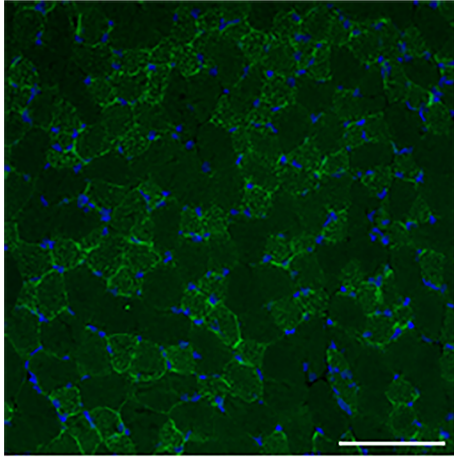


EDL
28 d

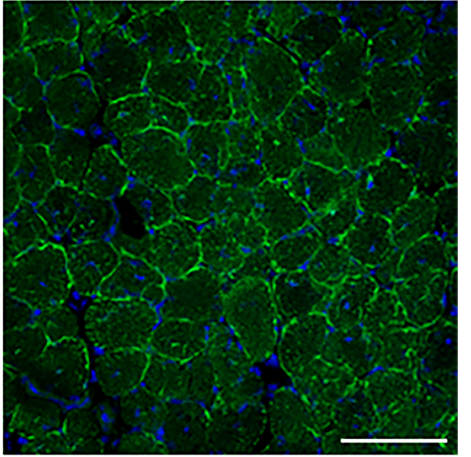
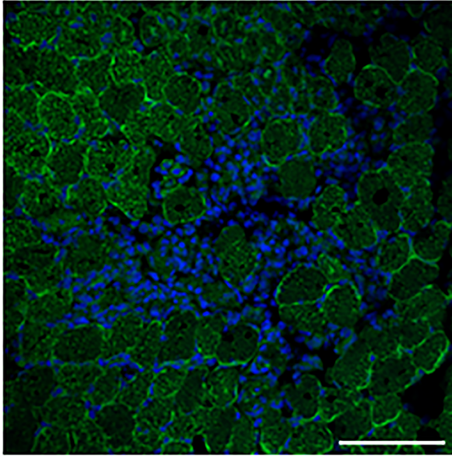
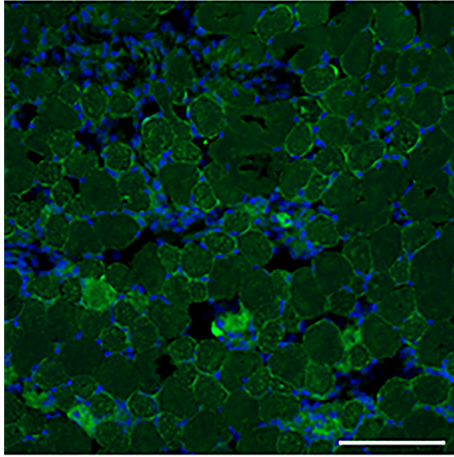
SOL
28 d

SOL
70 d

WT



mdx



mdx
tau

